Chapter 7
Targeted Nanoparticles

7.0 MATERIALS AND METHODS

7.1 Materials

Ethyl-3-dimethyl amino propyl carbodiimide (EDC) and N-hydroxysuccinimide (NHS) were purchased from H.B. Chemical, Vadodara, India.

7.2 Equipments

- High Speed Centrifuge (Sigma 3K30, Germany)
- Particle Size Analyzer 3000 HS (Zeta Sizer Nano Series, Malvern Instruments, UK)
- Transmission Electron Microscope (TEM, Philips, Technai 20, Holland)
- SDS-PAGE electrophoresis chamber (Genaxy Scientific Pvt. Ltd., USA)
- GelDoc™ XR^+ Imaging System (BioRad, USA)

7.3 Preparation scFv EGFR-DTX-HSA-NPs (DTX-HSA-INPs) and scFvEGFR-VBT-HSA-NPs (VBT-HSA-INPs)

To formulate immunonanoparticles (INPs), scFv EGFR was conjugated to the optimized DTX-HSA-NPs and VBT-HSA-NPs by crosslinking carboxyl groups on the surface of nanoparticles with amino groups of the scFv EGFR by ethyl-3-dimethyl amino propyl carbodiimide (EDC). 50-200 µg (50, 100, 150 and 200 µg) of the purified scFv EGFR in 500 µL of purified water were added to 500 µL of nanoparticle suspension in presence of EDC (0.6 mg) and N-hydroxysuccinimide (1.2 mg) on a rotating shaker. The nanoparticles were incubated with scFv EGFR for 6-24 h (6, 12, 18 and 24 h) and again purified by threefold centrifugation and redispersion. Unconjugated scFv EGFR was determined by BCA protein estimation assay.

7.3.1 Carbodiimide Reaction Principle

Carbodiimide compounds provide the most popular and versatile method for crosslinking of carboxylic acids (–COOH) present in proteins and many other biomolecules. The most readily available and commonly used carbodiimides are the water-soluble EDC for aqueous crosslinking and the water-insoluble DCC for non-aqueous organic synthesis methods. Carbodiimides work by activating carboxyl groups for direct reaction with primary amines via amide bond formation. Because no portion of their chemical structure becomes part of the final bond between conjugated molecules, carbodiimides are considered zero-length carboxyl-to-amine crosslinkers.

The ability to crosslink primary amines to carboxylic acid groups using EDC is a powerful and versatile tool for crosslinking peptides and proteins. Peptides and proteins contain both primary amines and carboxylic acids (N- and C-termini, respectively, as well as in the side-chain of certain amino acids). Thus, EDC enables peptides and proteins to be easily conjugated to one another or to any compounds or solid surfaces that bear either carboxyl or amino groups (1, 2).

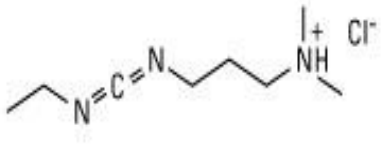

EDC
1-Ethyl-3-(3-dimethylaminopropyl)carbodiimide • HCl
MW 191.70
Spacer Arm 0.0 Å

7.3.2 EDC Reaction Chemistry

EDC reacts with carboxylic acid groups to form an active O-acylisourea intermediate that is easily displaced by nucleophilic attack from primary amino groups in the reaction mixture. The primary amine forms an amide bond with the original carboxyl group, and an EDC by-product is released as a soluble urea derivative. The O-acylisourea intermediate is unstable in aqueous solutions; failure to react with an amine results in hydrolysis of the intermediate, regeneration of the carboxyls, and the release of an N-unsubstituted urea (3, 4).

N-hydroxysuccinimide (NHS) or its water-soluble analog (Sulfo-NHS) is often included in EDC coupling protocols to improve efficiency or create dry-stable (amine-reactive) intermediates. EDC couples NHS to carboxyls, forming an NHS ester that is considerably more stable than the O-acylisourea intermediate while allowing for efficient conjugation to primary amines at physiologic pH (5).

7.4 Characterization of DTX-HSA-INPs and VBT-HSA-INPs

The prepared INPs were further analysed for mean particle size, % drug content, and Immunoreactivity. Prepared INPs were analyzed by SDS-PAGE to confirm the conjugation of scFv EGFR to nanoparticles. BCA estimation was performed to evaluate the unconjugated scFv EGFR.

7.4.1 Particle Size

Particle size and polydispersity index of the INPs were determined using a Malvern Zetasizer. Each sample was diluted ten times with filtered double distilled water to avoid multi-scattering phenomena and placed in disposable sizing cuvette. Analysis was performed in triplicate and the results were expressed as mean ± SD.

7.4.2 Transmission Electron Microscopy (TEM)

TEM is useful since it allows particles much smaller than 1 µm to be measured. In present work, TEM analysis was performed by Philips Technai 20 instrument. NPs were dispersed in distilled water and drop of redispersed NPs were placed on carbon coated copper grid. This copper grid was fixed into sample holder and placed in vacuum chamber of transmission electron microscope and observed under low vacuum.

7.4.3. *In-vitro* drug release

The *in vitro* drug release for DTX-HSA-INPs was carried out by dialysis bag technique as per **section 4.7.7** except DTX-HSA-NPs formulation was replaced with DTX-HSA-INPs. While the *in vitro* drug release for VBT-HSA-INPs was carried out as per **section 5.7.6** except VBT-HSA-NPs was replaced with VBT-HSA-INPs.

7.4.4 Stability Studies

The stability of DTX-HSA-INPs and VBT-HSA-INPs in terms of drug content and particle size distribution was monitored for 3 months at 2-8 °C and room temperature (25 °C). Periodically, samples were withdrawn and the particle size and drug content was determined.

7.4.5 SDS-PAGE analysis of scFv EGFR, NPs and INPs

The SDS-PAGE analysis was performed to determine the conjugation of scFv EGFR to NPs. SDS PAGE analysis protocol given in **Section 6.6.5.1 and 6.6.5.2**

7.5 Result and Discussion

7.5.1 Conjugation Reaction

scFv EGFR was successfully conjugated to the optimized DTX-HSA-NPs and VBT-HSA-NPs by crosslinking carboxyl groups on the surface on nanoparticles with amino groups of the scFv EGFR mediated by ethyl-3-dimethyl amino propyl carbodiimide (EDC). By BCA protein estimation assay it was found that around 120 µg

and 170 µg of the purified scFv EGFR was conjugated to 500 µL of nanoparticle suspension in presence of EDC of DTX-HSA-NPs and VBT-HSA-NPs respectively. 6 h incubation time was found sufficient for the conjugation of scFv EGFR to NPs and conjugation efficiency was not increased further by increase in incubation time.

7.5.2 Particle size

The particle size of optimized DTX-HSA-INPs and VBT-HSA-INPs was found 160.7 ± 5.5 nm and 164.5 ± 5.2 nm respectively. Results of particle size shown in **Figure 7.1 and Figure 7.2** respectively.

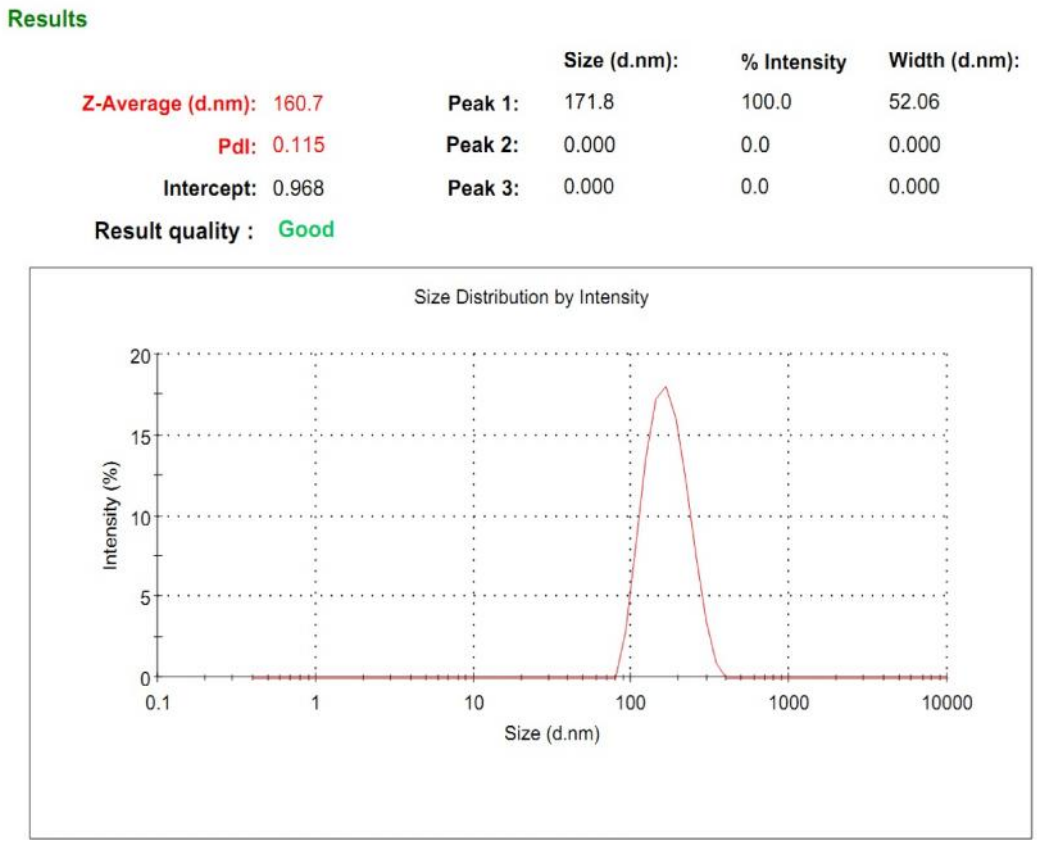

Figure 7. 1 Particle size distributions of optimized DTX-HSA-INPs

Figure 7. 2 Particle size distributions of optimized VBT-HSA-INPs

7.5.3 Transmission Electron Microscopy (TEM)

TEM imaging of optimized DTX-HSA-INPs and VBT-HSA-INPs exhibit a spherical shape without aggregation as shown in **Figure 7.3 and Figure 7.4** respectively. The diameters of INPs were in the range of 150-200 nm similar to particle size results obtained by Malvern Zetasizer.

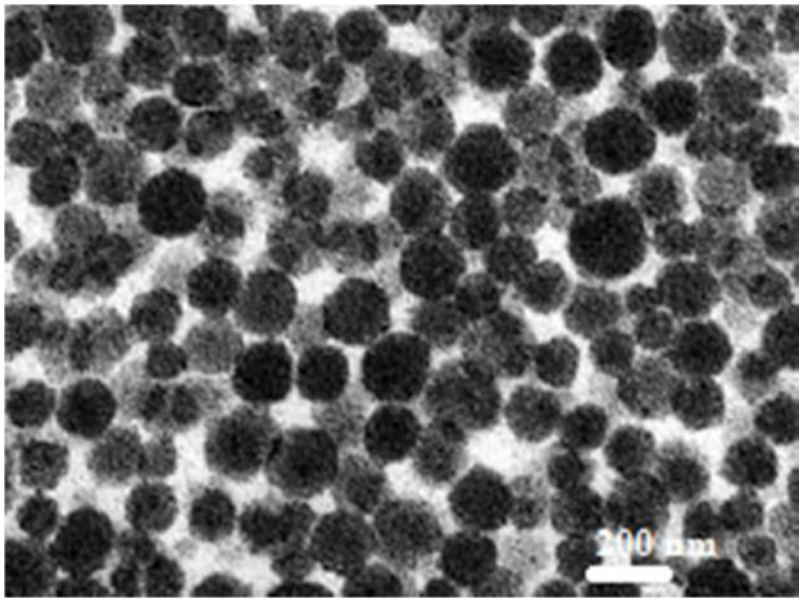

Figure 7. 3 TEM images of DTX-HSA-INPs

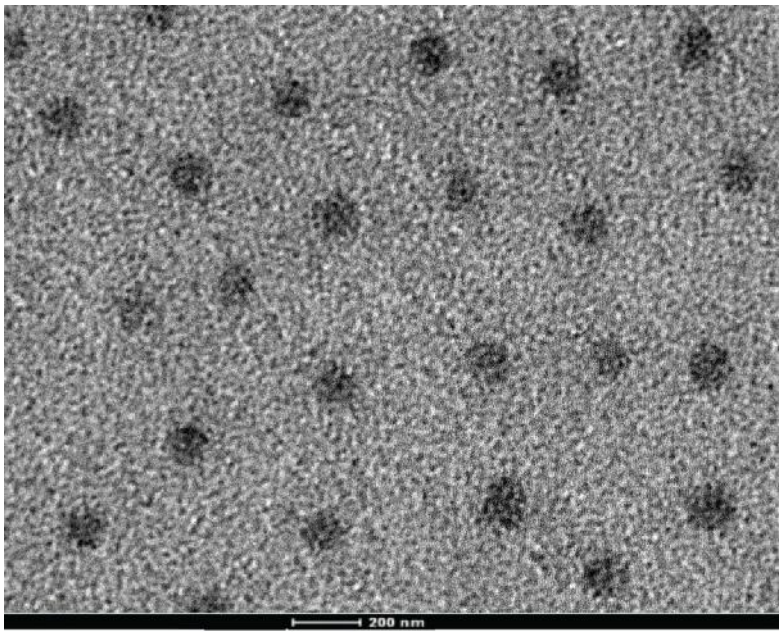

Figure 7. 4 TEM images of VBT-HSA-INPs

7.5.4 *In vitro* drug release

7.5.4.1 DTX-HSA-INPs

In vitro drug release studies were carried out for both plain DTX solution and for DTX-HSA-INPs by diffusion method for 24 h and results were compared by different kinetic models. The results of in-vitro drug release studies have shown that after the end of 8 h, 96.84±1.132 % of the drug was released from plain drug dispersion compared to 42.36 ± 1.342 % from DTX-HSA-INPs while at the end of 24 h, 65.38 ± 2.113 % of the drug was released from the DTX-HSA-INPs indicating prolonged release of drug from DTX-HSA-INPs. After application of different drug release kinetics models, it was observed that the DTX-HSA-INPs followed the Korsmeyer Peppas model because R^2 value (0.9873) which was nearer to 1 and having n value of 0.5746 indicating that drug transport mechanism is non-Fickian transport. DTX-HSA-INPs shown slower drug release as compared to DTX-HSA-NPs may be due to scFv conjugation. *In vitro* drug release data for plain DTX solution and DTX-HSA-INPs given in **Table 7.1** and Drug release pattern shown in **Figure 7.5**.

Table 7. 1 *In vitro* drug release data for plain DTX solution and DTX-HSA-INPs.

Time (h)	Cumulative% Drug Release (Mean ± SD)*	
	Plain drug dispersion	DTX-HSA-INPs
0.5	16.2 ± 0.215	7.21 ± 0.382
1	29.47 ± 0.967	12.19 ± 0.654
2	43.12 ± 1.312	19.32 ± 0.845
4	75.36 ± 1.415	27.59 ± 1.413
6	85.34 ± 1.115	31.21 ± 1.567
8	96.84 ± 1.132	42.36 ± 1.342
12	--	53.08 ± 1.632
24	--	65.38 ± 2.113

* The experiment was performed in triplicate (n=3)

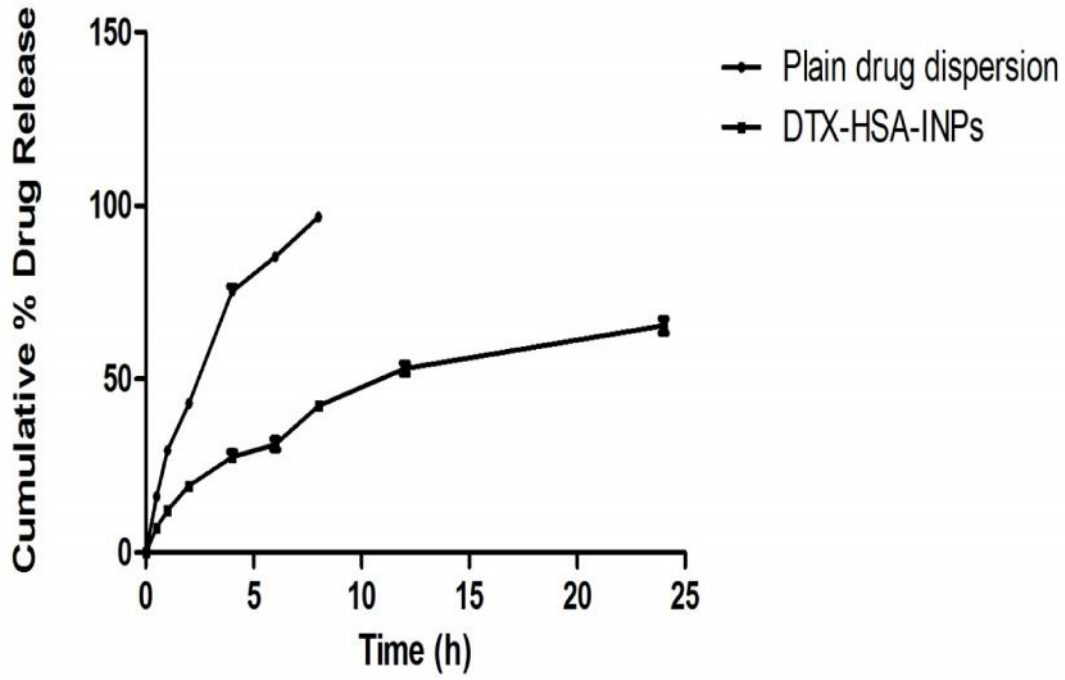

Figure 7. 5 *In vitro* drug release pattern of DTX-HSA-INPs

7.5.4.2 In vitro drug release

The *in vitro* drug release studies of VBT-HSA-INPs were carried out in trypsin phosphate buffered saline (pH 7.4) by diffusion method for 60 h and the results were compared by different kinetic models. An initial burst of more than 60% of the plain VBT in first 6 h was observed then a slow release up to 24 h. A cumulative release

reached 96% for plain VBT in 24 h, while VBT-HSA-INPs showed a slow release of drug up to 60 h, releasing approximately 82% of VBT. It is evident that the sustained release of drug from VBT-HSA-INPs will provide a better therapeutic efficacy than plain VBT. After application of different drug release kinetics models, it was observed that the VBT-HSA-INPs followed the Korsmeyer Peppas model because R^2 value (0.9401) which was nearer to 1 and having n value of 0.3931 indicating that drug transport mechanism is Fickian diffusion. VBT-HSA-INPs shown slower drug release as compared to VBT-HSA-NPs may be due to scFv conjugation. *In vitro* drug release data for plain VBT solution and VBT-HSA-INPs given in **Table 7.2** and Drug release pattern shown in **Figure 7.6**.

Table 7. 2 *In vitro* drug release data for plain VBT and VBT-HSA-INPs

Time (h)	Cumulative% Drug Release (Mean ± SD)*	
	Plain drug dispersion	VBT-HSA-INPs
0.5	15.9±0.155	9.97 ± 0.756
1	28.34±0.765	16.54 ± 0.831
2	41.72±1.123	26.93 ± 0.915
4	51.73±1.514	35.12 ± 1.570
6	60.78±1.432	43.89 ± 1.490
8	76.81±1.321	44.67 ± 1.621
12	88.42±1.563	52.82 ± 1.456
24	96.34±1.234	57.60 ± 1.431
36	-	62.13 ± 1.376
48	-	72.34 ± 2.487
60	-	82.17 ± 2.364

* The experiment was performed in triplicate (n=3)

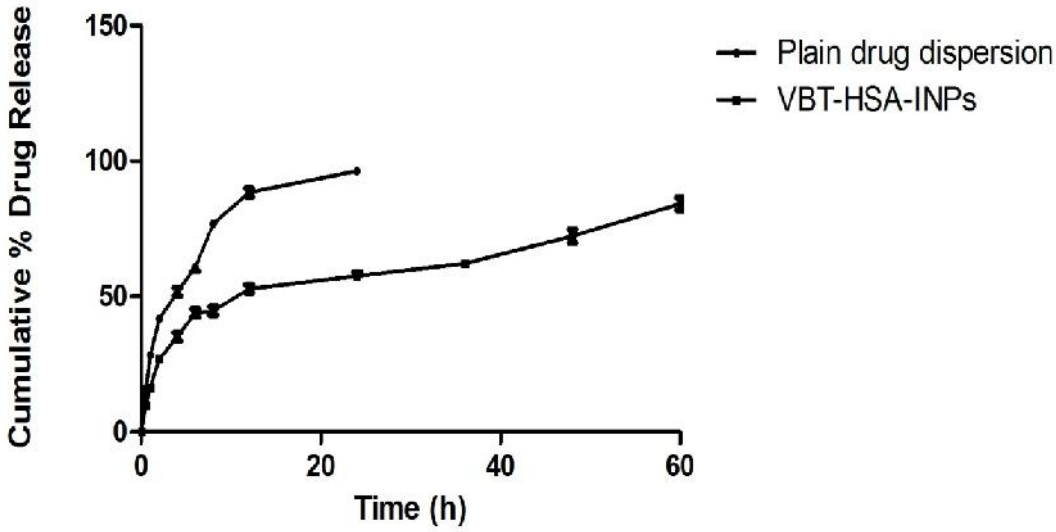

Figure 7. 6 *In vitro* drug release pattern of DTX-HSA-INPs

7.5.5 Stability of DTX-HSA-INPs and VBT-HSA-INPs

Stability study results of DTX-HSA-INPs and VBT-HSA-INPs for drug content and particle size are given in **Table 7.3** and **Table 7.4** and comparative graphs were shown in **Figure 7.7** and **Figure 7.8** respectively.

Table 7. 3 Stability data of DTX-HSA-INPs at different temperature conditions.

Temperature Condition	Sampling Time (days)	Particle size (nm.)* Mean ± SD	% Assay* Mean ± SD
Initial	0	160.7 ± 5.5	99.77±0.087
Room Temperature	15	169.3 ± 4.7	99.38±0.015
	30	175.4 ± 5.4	99.10±0.060
	45	179.0 ± 4.9	98.74±0.059
	60	197.0 ± 4.6	98.52±0.040
	90	221.0 ± 5.2	98.18±0.061
2-8îC	15	161.2 ± 4.2	99.68±0.060
	30	166.4 ± 4.6	99.64±0.045
	45	170.7 ± 4.1	99.52±0.065
	60	172.1 ± 4.9	99.43±0.067
	90	174.3 ± 3.7	99.37±0.034

* The experiment was performed in triplicate (n=3)

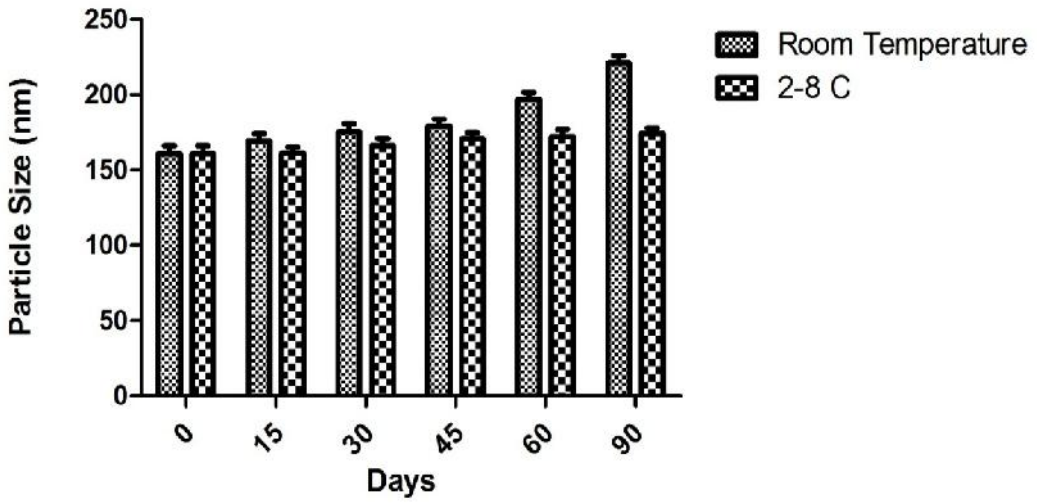

Figure 7. 7 Comparative changes in particle size of DTX-HSA-INPs with different temperature conditions during stability

Table 7. 4 Stability data of VBT-HSA-INPs at different temperature conditions

Temperature Condition	Sampling Time (days)	Particle size (nm)* (Mean ± SD)	% Assay* (Mean ± SD)
Initial	0	164.5 ± 5.2	99.76 ±0.067
Room Temp.	15	171.5 ± 3.9	99.53±0.031
	30	175.4 ± 4.9	99.23±0.021
	45	181.6 ± 4.7	98.76±0.043
	60	191.7 ± 3.6	98.64±0.055
	90	210.6 ± 3.9	98.07±0.048
2-8îC	15	166.2 ± 3.1	99.61±0.066
	30	169.5 ± 3.6	99.49±0.045
	45	172.7 ± 3.7	99.27±0.056
	60	174.5 ± 3.4	99.21±0.068
	90	175.6 ± 3.5	99.10±0.034

* The experiment was performed in triplicate (n=3)

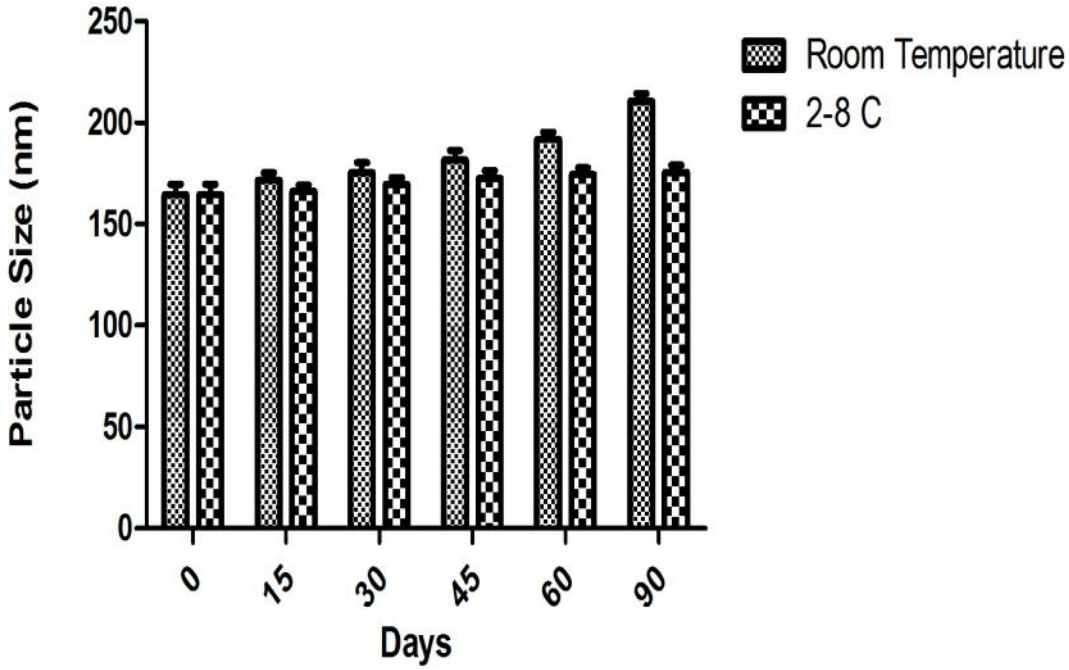

Figure 7. 8 Comparative changes in particle size of VBT-HSA-INPs with different temperature conditions during stability.

It was observed that DTX-HSA-INPs and VBT-HSA-INPs were stable over the period of 3 months. The DTX-HSA-INPs and VBT-HSA-INPs showed physical stability for the period of 3 months at 2-8°C. The drug content at room temperature was found to decrease during storage and the particle size was also increased above 220 nm, which was not desirable. Hence, Room Temperature is not suitable for storage of DTX-HSA-INPs and VBT-HSA-INPs while storage at 2 -8°C no significant difference was observed in the particle size and drug content of INPs after 3 months at refrigerated conditions indicating its suitability for storage at 2 -8°C.

7.5.6 SDS-PAGE analysis of scFv EGFR, NPs and INPs

Sample 1 (Albumin NPs), Sample 2 (scFv EGFR), protein marker (27, 36, 43, 56, 66, 97 and 116 kDa), Sample 3 (Mixture of NPs and scFv EGFR), Sample 4 (INPs) respectively. In Sample 1, one band was observed at molecular weight of ~66 kDa corresponding to albumin NPs. In Sample 2, one band was observed at molecular weight below 27 kDa corresponding 25 kDa scFv EGFR. In Sample 3, two bands were observed at molecular weight of ~66 kDa corresponding to albumin NPs and below 27

kDa corresponding 25 kDa scFv EGFR indicates absence of conjugation in physical mixture. The conjugation of scFv-EGFR over NPs can be confirmed by disappearance of both the scFv-EGFR and albumin NPs band and appearance of new band corresponding to INPs in Sample 4 (7). We observed very big and well spreaded new band between 66 and 97 kDa (around 90 kDa) indicating the formation of INPs shown in **Figure 7.9.**

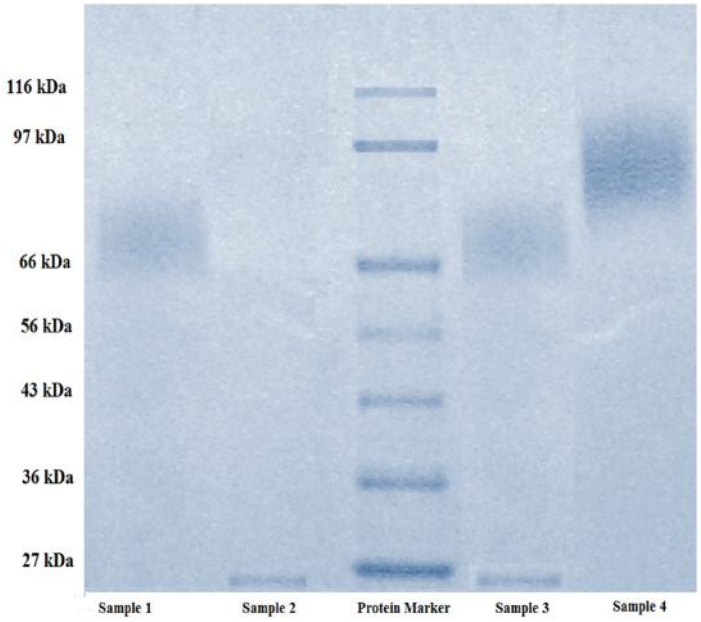

Figure 7. 9 SDS Page Analysis for confirmation of conjugation reaction forming INPs

7.6 References

1. Liu L, Deng D, Xing Y, Li S, Yuan B, Chen J, et al. Activity analysis of the carbodiimide-mediated amine coupling reaction on self-assembled monolayers by cyclic voltammetry. Electrochimica Acta. 2013;89:616-22.
2. Parinaz AS, Tam KC, Berry RM. Surface modified nanocrystalline cellulose and uses thereof. Google Patents; 2014.
3. Calabro A, Gross R, Darr A. Hydroxyphenyl cross-linked macromolecular network and applications thereof. Google Patents; 2005.
4. Lellouche JP, Goldman D. A "Growth from surface" Methodology for the Fabrication of Functional Dual Phase Conducting Polymer polypyrrole/polycarbazole/Polythiophene (CP/polyPyr/polyCbz/PolyTh)-Carbon Nanotube (CNT) Composites of Controlled Morphology and Composition - Sidewall versus End-Selective PolyTh Deposition. Google Patents; 2011.
5. Neamati N, Dayam R. Integrin-binding small molecules. Google Patents; 2011.
6. Vigor KL, Kyrtatos PG, Minogue S, Al-Jamal KT, Kogelberg H, Tolner B, et al. Nanoparticles functionalized with recombinant single chain Fv antibody fragments (scFv) for the magnetic resonance imaging of cancer cells. Biomaterials. 2010 Feb;31(6):1307-15.
7. Nielsen UB, Kirpotin DB, Pickering EM, Hong K, Park JW, Refaat Shalaby M, et al. Therapeutic efficacy of anti-ErbB2 immunoliposomes targeted by a phage antibody selected for cellular endocytosis. Biochim Biophys Acta. 2002 Aug 19;1591(1-3):109-18.